Finite-size corrections in the bosonic algebraic approach to two-dimensional systems

P. Pérez-Fernández* and José M. Arias†
Departamento de Física Atómica, Molecular y Nuclear, Facultad de Física, Universidad de Sevilla, Apartado 1065, E-41080 Sevilla, Spain

J. E. García-Ramos‡ and F. Pérez-Bernal§
Departamento de Física Aplicada, Facultad de Ciencias Experimentales, Universidad de Huelva, Campus del Carmen, Avenida de las Fuerzas Armadas s/n E-21071 Huelva, Spain

(Received 7 March 2011; published 30 June 2011)

Analytical results beyond the mean-field-limit approximation for several observables of the two-dimensional limit of the vibron model are presented. Finite-size scaling exponent values are also analytically derived. The computed corrections and scaling exponents are compared to numerical calculations for this algebraic model, based on a bosonic u(3) spectrum-generating algebra, obtaining good agreement.

DOI: 10.1103/PhysRevA.83.062125 PACS number(s): 03.65.Fd, 05.70.Fh, 05.70.Jk, 33.20.Vq

I. INTRODUCTION

Researchers from widely different fields of physics, from condensed-matter to high-energy particle physics, show significant interest in the study of quantum phase transitions (QPTs) as zero-temperature phase transitions between different phases of a system. In particular, special attention has been drawn to the transitions between different geometrical limits of algebraic models. The pioneer work in this field was carried out by Gilmore [1], who coined the term ground-state transitions to refer to the qualitative changes that a system's ground-state wave function undergoes upon small changes in the Hamiltonian parameters in the vicinity of their critical value.

The algebraic approach, based on the concept of spectrum-generating algebra, has given rise to simple and insightful approximations for the study of different physical systems. Nuclear structure is one of the branches of physics where this approach has gained more momentum, and the interacting boson model (IBM) [2] has become a standard tool in this field, offering a simple model that fits a wide range of nuclei well. A very similar formalism, the vibron model, has also proved useful in the modeling of molecular structure [3]. A particularity of the algebraic approach is the existence of dynamical symmetries, which are situations associated with a particular chain of algebras that terminates in the system's symmetry algebra. Dynamical symmetries provide easy-to-handle limiting cases, usually with a clear physical interpretation and an analytical energy formula [2–5]. Each dynamical symmetry can be mapped to a geometrical configuration of the system. The system's Hamiltonian can be defined in such a way that, according to the values of one or several control parameters, it can be made of Casimir or invariant operators belonging exclusively to one of the available dynamical symmetries. In this way, varying the control parameter values, the Hamiltonian encompasses the full gamut of intermediate situations. This is the main reason why algebraic models provide a handle on the study of precursors of QPTs in mesoscopic systems [6].

The QPTs, also called, in this context, ground-state transitions and shape-phase transitions, take place when small changes in the control parameters around a critical value enforce qualitative changes in the nature of the system's ground state. Recent reviews of QPTs in algebraic models can be found in Refs. [7–9].

In this paper, we deal with the two-dimensional (2D) limit of the vibron model. The vibron model, originally presented in Ref. [10], is an algebraic model based on the spectrum-generating algebra u(4). This approach is appropriate for the modeling of three-dimensional systems and has mostly been employed to model rotational and vibrational molecular spectra of diatomic [10,11] and polyatomic [12,13] molecular species, treating molecular degrees of freedom as collective excitations in a bosonic space (vibrons) [3]. The one-dimensional (1D) limit of the model [14] has been used to decouple vibrations from rotations, permitting us to take full advantage of the discrete molecular symmetry [15].

The 1D limit of the vibron model is specially suited to deal with stretching vibrations. However, the study of the bending dynamics of linear and quasilinear molecules implies the simultaneous consideration of rotational and vibrational degrees of freedom. This is a 2D problem, for which the 2D limit of the vibron model constitutes an appropriate framework using the u(3) Lie algebra as a spectrum-generating algebra. Originally presented in Ref. [16], this model has proved useful for modeling the vibrational bending excitation spectrum [17] and line intensities [18] of quasilinear and nonrigid molecular species. A recent reference [19] presents a detailed account of this algebraic model, both from a quantal and a classical perspective. Hereafter, we will refer to the 2D limit of the vibron model as the u(3) model.

Apart from the application to the modeling of vibrational bending dynamics, the u(3) model has been applied to other systems. On one hand, it has been proposed in the realm of high-T_c superconductors based on s-d wave pairing in 2D systems [20–22]. On the other hand, the u(3)-based algebraic model is a convenient playground to study excited-state QPTs (ESQPTs) [23–27]. In this latter case, the transition does not take place on the system's ground state upon a change of a control parameter but on excited states of the system as

*pedropf@us.es
†ariasc@us.es
‡enrique.ramos@dfaie.uhu.es
§francisco.perez@dfaie.uhu.es

the excitation energy increases. With regard to the ESQPT topic, the u(3) model permits access to an interesting aspect of molecular systems: the appearance of monodromy in vibrational bending spectroscopy [19,27]. The possibility of finding experimental realizations of such transitions in the field of molecular spectroscopy, on account of the experimental access to highly excited molecular species, has further bolstered this line of research. The vibrational bending spectrum of water in its electronic ground state is one of the systems where monodromy effects have been recorded experimentally [28,29].

The study of the phase diagram associated with the different dynamical symmetries of an algebraic model Hamiltonian takes place in the mean-field limit, also called the thermodynamic or large-N limit. This limit is obtained using a variational approach, valid up to $1/N$ order, where N is related to the system's size and becomes exact when $N \to \infty$. An important advantage of algebraic models is that they allow the study of scaling laws and finite-size effects [6]. However, in order to compare numerically obtained results with analytical finite-size corrections, it is necessary to go beyond the mean-field limit.

The main motivation of the present paper is to explore the finite-size corrections induced in several observables of interest for the 2D limit of the vibron model. In order to do so, we combine a Holstein-Primakoff expansion with a Bogoliubov transformation in the different geometrical phases of the system. The phases are defined according to the analysis of the system in the thermodynamic limit. This approach has proved useful for two-level boson systems with a spectrum-generating algebra u$(2L+2)$ with $L = 0,1,2,\ldots$ [30,31]. The present case is the simplest case with a half-integer value of L, $L = 1/2$: a two-level model with a scalar boson as a ground state and a doubly degenerate upper level, which in our case, is represented by two Cartesian bosons. The generators of the u(3) dynamical algebra are the bilinear products of a creation times an annihilation boson. The analytical finite-size corrections obtained in the present paper should match the numerical calculations presented in Ref. [19]. In the Appendix, we also present a connection between this paper and the results presented by Dusuel *et al.* in Ref. [30].

The outline of the present paper is as follows. The prefatory remarks in this section are followed, in Sec. II, by an abridged explanation of the basic facts about the u(3) model, the definition of a model Hamiltonian and several observables of interest, and the results obtained in the mean-field limit. Section III is devoted to the derivation of the analytical finite-size corrections to the mean-field limit. This section is followed by Sec. IV, where the analytical results derived in the previous section are compared to numerical results. The analytical derivation of the scaling properties of the model with the system's size is presented in Sec. V. Finally, Sec. VI includes a brief summary of the main results presented as well as our concluding remarks.

II. THE u(3) ALGEBRAIC MODEL HAMILTONIAN AND ITS CLASSICAL LIMIT

The modeling of n-dimensional many-body systems using a spectrum-generating algebra u$(n+1)$ provides an effective description of a large variety of systems. In this section, we briefly review the u(3) algebraic approach to 2D systems [16,19].

A. The bosonic u(3) algebra for 2D systems

The bosonic u(3) Lie algebra for 2D systems is built from a two-level boson model. The lower level is associated with a scalar boson $\sigma^\dagger$, and the upper level is associated with two degenerate Cartesian bosonic operators $\{\tau_x^\dagger, \tau_y^\dagger\}$. The commutation relations between creation and annihilation operators are

$$[\sigma,\sigma^\dagger] = 1, \quad [\tau_i,\tau_j^\dagger] = \delta_{i,j}, \quad [\tau_i,\sigma^\dagger] = 0, \quad i,j = x,y. \tag{1}$$

All other commutators are zero. It is convenient to introduce circular bosons [19],

$$\tau_\pm^\dagger = \mp\frac{\tau_x^\dagger \pm i\tau_y^\dagger}{\sqrt{2}}, \tag{2a}$$

$$\tau_\pm = \mp\frac{\tau_x \mp i\tau_y}{\sqrt{2}}. \tag{2b}$$

The nine u(3) generators are the bilinear products of creation and annihilation operators. They can be written as [16]

$$\begin{gathered}\hat{n} = \tau_+^\dagger\tau_+ + \tau_-^\dagger\tau_-, \quad \hat{n}_s = \sigma^\dagger\sigma, \quad \hat{l} = \tau_+^\dagger\tau_+ - \tau_-^\dagger\tau_-,\\ \hat{D}_+ = \sqrt{2}(\tau_+^\dagger\sigma - \sigma^\dagger\tau_-), \quad \hat{D}_- = \sqrt{2}(-\tau_-^\dagger\sigma + \sigma^\dagger\tau_+),\\ \hat{Q}_+ = \sqrt{2}\,\tau_+^\dagger\tau_-, \quad \hat{Q}_- = \sqrt{2}\,\tau_-^\dagger\tau_+,\\ \hat{R}_+ = \sqrt{2}(\tau_+^\dagger\sigma + \sigma^\dagger\tau_-), \quad \hat{R}_- = \sqrt{2}(\tau_-^\dagger\sigma + \sigma^\dagger\tau_+).\end{gathered} \tag{3}$$

The operator $\hat{l}$ is the angular momentum in 2D, as one can easily see once it is expressed in terms of Cartesian boson operators.

There are two possible dynamical symmetries that conserve 2D angular momentum. Both start in the u(3) dynamical algebra and end in the so(2) symmetry algebra,

$$\text{u(3)} \supset \text{u(2)} \supset \text{so(2) Chain I}, \tag{4a}$$

$$\text{u(3)} \supset \text{so(3)} \supset \text{so(2) Chain II}. \tag{4b}$$

The system's symmetry algebra is so(2), which corresponds to rotations on a plane, and the associated quantum number is l. Due to the 2D nature of the system, l is not an angular momentum but a component of it and can take both positive and negative (or zero) values.

Each dynamical symmetry conveys a basis and an analytical energy formula. Numerical calculations in the present paper have been carried out using the TRIAT_U3 package [32] that makes use of the cylindrical oscillator basis, associated with dynamical symmetry I. A detailed discussion of both dynamical symmetries can be found in Ref. [19].

The definition of a simple Hamiltonian that contains the main physical ingredients of the model implies the consideration of Casimir or invariant operators of the chains under study. We consider the first-order Casimir operator of u(2) and the second-order Casimir operator of so(3),

$$\hat{C}_1[\text{u(2)}] = \hat{n}, \quad \hat{C}_2[\text{so(3)}] = \hat{W}^2 = (\hat{D}_+\hat{D}_- + \hat{D}_-\hat{D}_+)/2 + \hat{l}^2. \tag{5}$$

The so(3) Casimir operator $\hat{W}^2$ can be replaced by the pairing operator,

$$\hat{P} = N(N+1) - \hat{W}^2, \tag{6}$$

where the total number operator $\hat{N} = \hat{n}_s + \hat{n}$ has been replaced by its value N due to the fact that we consider systems with a fixed number of bosons.

B. Model Hamiltonian

Phase transitions in algebraic models can be studied by considering a general Hamiltonian written in terms of Casimir operators of all chains [1,33,34]. However, for the sake of simplicity, invariant operators in subalgebras common to all the dynamical symmetries under study are not included, and an essential Hamiltonian is built considering one operator for each dynamical symmetry. Therefore, ground-state phase transitions in the u(3) approach can be studied by considering the model Hamiltonian,

$$\hat{\mathcal{H}} = \varepsilon \left[(1-\xi)\hat{n} + \frac{\xi}{N-1}\hat{P} \right]. \tag{7}$$

We have made use of Eqs. (5) and (6), put the overall energy scale ε in front, and introduced the dimensionless control parameter $\xi \in [0,1]$. At $\xi = 0$, the system is in phase I—i.e., the eigenvalues and eigenstates of $\hat{\mathcal{H}}$ are those of the dynamical symmetry I—while at $\xi = 1$, the system is in phase II—i.e., the eigenvalues and eigenstates are those of dynamical symmetry II. The factor $1/(N-1)$ is a normalization factor, introduced to obtain a well-behaved Hamiltonian in the large-N limit, taking into account that the pairing operator $\hat{P}$ is a two-body operator, while $\hat{n}$ is a one-body operator. One-body operators scale as N, and two-body operators scale as $N(N-1)$ [33]. This model Hamiltonian has proved useful in the modeling of the bending dynamics of several molecular species [17,18], while the quantal and classical properties of its associated phase diagram can be found in Ref. [19]. This Hamiltonian is similar to the generalization of the IBM consistent-Q Hamiltonian proposed in Ref. [30]. As shown in the Appendix, we can link our model Hamiltonian and the general boson-pairing Hamiltonian in Ref. [30].

Four possible physical scenarios can be distinguished with the model Hamiltonian (7) [17,19]:

(1) Rigidly linear case, $\xi = 0$. The spectrum corresponds to a 2D truncated harmonic oscillator with the corresponding l degeneracy (dynamical symmetry I).

(2) Quasilinear case, $0 < \xi \leqslant 0.2$. In this case, the main feature is the appearance of *positive* anharmonicity. The degeneracy in l is broken in a particular way with smaller energy values for increasing values of l.

(3) Quasibent case, $0.2 < \xi < 1$. This situation is characterized by the appearance of an anharmonicity that is negative for the low-lying states and becomes positive at high energy. As in the previous case, the l degeneracy is broken. In molecular physics, this situation has long since been known as the Dixon dip [35].

(4) Rigidly bent case, $\xi = 1$. The spectrum is that of a 2D truncated rovibrator (dynamical symmetry II). The l quantum number corresponds to the angular momentum projection on the figure axis, usually labeled K, with rotational bands on top of a vibrational head.

C. Mean-field limit

In order to understand whether or not the variations seen numerically in some quantities as a function of the control parameter are indeed related to phase transitions, it is convenient to make use of an algorithm introduced by Gilmore [1], Gilmore and Feng [33], and Feng *et al.* [34]. This formalism provides the limit $N \to \infty$ (called classical, thermodynamic, or mean-field limit) of the model in terms of geometrical or shape variables. Such variables are used to define the system's phase diagram. The limit is called classical because the algorithm produces a classical Hamiltonian in terms of coordinates (and momenta), upon which, a Landau analysis of the phase transition can be performed. The mean-field name stems from a fact shown long ago by Gilmore and Feng [33]: By minimizing the ground-state expectation value of a Hamiltonian that is regular in the large-N limit, one obtains an upper limit to the ground-state energy per particle E_0/N, which converges to the exact energy when $N \to \infty$. A detailed discussion of the application of this algorithm to the u(3) algebra can be found in Ref. [19].

In making use of the algorithm, we use projective coherent states that define a normalized intrinsic ground state,

$$|[N];0;r,\theta\rangle = \frac{1}{\sqrt{N!}}(b_c^\dagger)^N|0\rangle, \tag{8}$$

where r and θ are the polar coordinates associated with the Cartesian coordinates x and y, and $b_c^\dagger$ is the boson condensate,

$$b_c^\dagger = \frac{1}{\sqrt{1+r^2}}(\sigma^\dagger + x\tau_x^\dagger + y\tau_y^\dagger). \tag{9}$$

The coherent state (8) is the number-projected generalized coherent state of u(3) [2]. These coherent u(n) states were introduced by Gilmore [1] and others [36–38] in the context of nuclear physics (Lipkin-Meshkov-Glick quasispin model [39] and Arima-Iachello IBM [2]) and later in the context of molecular physics [40–42] (Iachello-Levine vibron model [3]). The coherent states (8) have been generalized to include excited states [42–44]. The boson condensate definition (9) is not unique; a different alternative, for the same bosonic u(3) algebra, can be found in Ref. [44].

The intrinsic state allows the expression in terms of classical coordinates and momenta of any operator built with the elements of the spectrum-generating algebra. It should be noted that the parameters in the coherent state, in general, are complex and represent both coordinates and momenta [41]. For the applications in this paper, we only consider the dependence on coordinates and, thus, set all momenta (p_r, p_θ) equal to zero.

The ground-state energy functional is the expectation value of the Hamiltonian in the intrinsic ground state,

$$E(r,\theta) \equiv \langle [N];0;r,\theta|\hat{\mathcal{H}}|[N];0;r,\theta\rangle. \tag{10}$$

By minimizing $E(r,\theta)$ with respect to r and θ, one obtains an approximation for the exact ground-state energy, which is valid to order N [33].

The energy functional for the essential Hamiltonian (7) is trivially obtained from Eq. (10) [17,19]. The energy per

particle $\mathcal{E} = E/N$ is

$$\mathcal{E}_\xi(r) = \varepsilon\left[(1-\xi)\frac{r^2}{1+r^2} + \xi\left(\frac{1-r^2}{1+r^2}\right)^2\right]. \tag{11}$$

This energy functional does not depend on the polar angle θ, since the Hamiltonian is a scalar operator.

The minimization of the energy functional (11) reveals that there are two different geometric limits: symmetric (or linear) limit and deformed (or bent) limit. In the first case, the energy minimum is at the equilibrium value $r_e = 0$, while the second case implies that the minimum energy is attained for $r_e = \sqrt{(5\xi-1)/(3\xi+1)} \neq 0$. The symmetric phase takes place for control parameter values $\xi \leqslant \xi_c = 0.2$, while for values of $\xi > \xi_c = 0.2$, the deformed phase has a lower energy. When evaluated at $r = r_e$, the energy functional is

$$\mathcal{E}_\xi(r_e) = \begin{cases} \xi, & 0 \leqslant \xi \leqslant \xi_c, \\ \frac{-9\xi^2+10\xi-1}{16\xi}, & \xi_c < \xi \leqslant 1. \end{cases} \tag{12}$$

By evaluating the derivatives of $\mathcal{E}_\xi(r_e)$ with respect to ξ, one finds that the second derivative is discontinuous at $\xi = \xi_c$, and r_e can be taken as a classical order parameter [19]. According to Ehrenfest's classification scheme, the phase transition is of second order.

Several observables can be selected to study the phase transition, both at the large-N limit and for finite systems. In the present case, we select four observables that are of interest in the study of QPTs, and whose behavior, beyond the mean-field limit, has been studied for u$(2L+2)$ bosonic two-level systems in Ref. [30]. Numerical results for most of these observables in the u(3) boson model under study can be found in Ref. [19]. For the sake of completeness, we proceed to briefly review mean-field results. In Sec. III, we analytically derive the next order correction in N for the selected observables.

The four observables under study are the ground-state energy per particle ($\mathcal{E}_0$), the expectation value in the ground state of the number of Cartesian bosons per particle ($\langle\hat{n}\rangle/N$), the first excited-state energy gap ($\Delta_{1\text{ph}}$), and the transition probability between the ground state and the first excited state (T/N). The calculation in the mean-field limit of $\mathcal{E}_0$ and $\langle\hat{n}\rangle/N$ is immediate, and the results can be found in Ref. [19]. The ground-state energy per boson is given in Eq. (12), and the expectation value of the u(2) number operator is

$$\langle[N];0;r,\theta|\hat{n}|[N];0;r,\theta\rangle = N\frac{r_e^2}{1+r_e^2} = \begin{cases} 0, & 0 \leqslant \xi \leqslant \xi_c, \\ \frac{5\xi-1}{8\xi}, & \xi_c < \xi \leqslant 1. \end{cases} \tag{13}$$

The mean-field limit calculation of the other two observables implies an excited state, and it is slightly more involved. We proceed to briefly resume the results obtained for these two observables in the mean-field limit.

In order to calculate the mean-field limit of one-quantum excitations, we consider the possible bosonic excitations orthonormal to Eq. (9). There are, up to a phase, two possibilities,

$$b_1^\dagger = \frac{1}{r\sqrt{1+r^2}}(-r^2\sigma^\dagger + x\tau_x^\dagger + y\tau_y^\dagger), \tag{14a}$$

$$b_2^\dagger = \frac{1}{r}(y\tau_x^\dagger - x\tau_y^\dagger). \tag{14b}$$

The possible one particle-hole (1ph) excitations can be obtained replacing a condensate boson by an excited boson in Eq. (8),

$$|[N];i;r,\theta\rangle = \frac{1}{\sqrt{(N-1)!}}b_i^\dagger(b_c^\dagger)^{N-1}|0\rangle, \tag{15}$$

with $i = 1,2$. This procedure is known as the Tamm-Dancoff approximation (TDA) [42,43]. The 1ph energy excitation $\Delta_{1\text{ph}}^{(i)}$ is computed as

$$\Delta_{1\text{ph}}^{(i)} = \langle[N];i;r,\theta|\hat{\mathcal{H}}|[N];i;r,\theta\rangle - \langle[N];0;r,\theta|\hat{\mathcal{H}}|[N];0;r,\theta\rangle, \tag{16}$$

with $i = 1,2$. The energy gap obtained in the symmetric and deformed phases, for the two possible excitations (14), is

$$\Delta_{1\text{ph}}^{(1)} = \begin{cases} 1-3\xi, & 0 \leqslant \xi \leqslant \xi_c, \\ \frac{1}{4} + \frac{31}{8}\xi - \frac{1}{8\xi}, & \xi_c < \xi \leqslant 1, \end{cases} \tag{17a}$$

$$\Delta_{1\text{ph}}^{(2)} = \begin{cases} 1-3\xi, & 0 \leqslant \xi \leqslant \xi_c, \\ \frac{1-\xi}{2}, & \xi_c < \xi \leqslant 1. \end{cases} \tag{17b}$$

It is worth emphasizing that these results, at the TDA level, are not fully self-consistent mean-field results. The result (17b), obtained using the excited boson (14b), implies that this excitation becomes a spurious Goldstone boson in the deformed phase ($\xi > \xi_c$), associated with a rotation in the plane. This point is in good accordance with the well-known fact that there exists two degenerate vibrational degrees of freedom in the symmetric (linear) configuration that correlate to a vibrational plus a rotational degree of freedom in the deformed (nonlinear or bent) case. Note that, for $\xi < \xi_c$, the gap is the same in both cases, and the excitations are degenerate.

Therefore, a careful definition of this observable $\Delta_{1\text{ph}}$ is important. The appearance of a Goldstone boson in the distorted or broken phase ($\xi > \xi_c$) implies that the first excited state in the broken-symmetry phase corresponds to a state with two quanta of excitation in the symmetric phase. This can already be appreciated in the correlation energy diagrams in Ref. [19], and it is a general feature of the u$(2L+1)$-so$(2L+2)$ QPT as explained in Ref. [30]. In particular, when comparing to the numerical results presented in Ref. [19], the energy gap $\Delta_{1\text{ph}}$ does not correspond all the way, neither to the first vibrational energy gap, nor to the first rotational energy gap, denoted as $\Gamma_{u=1,\text{vib}}$ and $\Gamma_{l=1,\text{rot}}$ in Ref. [19]. In order to compare the present paper's results and the calculations published in Ref. [19], the $\Delta_{1\text{ph}}$ gap corresponds to $\Gamma_{l=1,\text{rot}}$ for $\xi < \xi_c$ and $\Gamma_{u=1,\text{vib}}$ for $\xi > \xi_c$.

The fourth observable considered is the transition probability between the ground state and the first excited state. We begin defining a transition operator in terms of the generators of the u(3) algebra. We select, as a candidate, the dipole transition

operator [16,18,19,30],

$$\hat{T}_{\pm} = \hat{D}_{\pm}, \tag{18}$$

and calculate the transition probability or transition intensity between states $|\psi_1\rangle$ and $|\psi_2\rangle$ as

$$I_{2\to 1} \propto \frac{1}{g_2}(|\langle\psi_2|\hat{T}_+|\psi_1\rangle|^2 + |\langle\psi_2|\hat{T}_-|\psi_1\rangle|^2), \tag{19}$$

where g_2 is a statistical factor that takes the initial-state degeneracy into account.

Following the notation in Ref. [30], we denote the transition intensity between the ground state (0_1) and the first excited state with angular momentum one (1_1) as T, and we normalize this observable by a factor of N. We assume that we cannot distinguish between negative and positive values of the vibrational angular momentum l. Therefore, if any of the involved states has a vibrational angular momentum different from zero, we add up the positive and negative l contributions.

As in the energy-gap case, there is a fundamental difference in the treatment of the symmetric and deformed regions [30]. To further clarify this point, we express the intrinsic bosons (9) and (14) in circular coordinates,

$$b_c^\dagger = \frac{1}{\sqrt{1+r^2}}\left(\sigma^\dagger - r\frac{e^{-i\theta}}{\sqrt{2}}\tau_+^\dagger + r\frac{e^{i\theta}}{\sqrt{2}}\tau_-^\dagger\right), \tag{20a}$$

$$b_1^\dagger = \frac{1}{\sqrt{1+r^2}}\left(-r\sigma^\dagger - \frac{e^{-i\theta}}{\sqrt{2}}\tau_+^\dagger + \frac{e^{i\theta}}{\sqrt{2}}\tau_-^\dagger\right), \tag{20b}$$

$$b_2^\dagger = \frac{i}{\sqrt{2}}(e^{i\theta}\tau_+^\dagger + e^{-i\theta}\tau_-^\dagger). \tag{20c}$$

In the symmetric phase, the equilibrium value of r is $r_e = 0$, and the intrinsic bosons are simplified to

$$b_c^\dagger = \sigma^\dagger, \tag{21a}$$

$$b_1^\dagger = -\frac{e^{-i\theta}}{\sqrt{2}}\tau_+^\dagger + \frac{e^{i\theta}}{\sqrt{2}}\tau_-^\dagger, \tag{21b}$$

$$b_2^\dagger = \frac{ie^{i\theta}}{\sqrt{2}}\tau_+^\dagger + \frac{ie^{-i\theta}}{\sqrt{2}}\tau_-^\dagger. \tag{21c}$$

In this case, $b_c^\dagger$ has zero angular momentum, while $b_1^\dagger$ and $b_2^\dagger$ are a mixture of $\tau_+^\dagger$ and $\tau_-^\dagger$. However, it is trivial to recombine the bosons defined in Eqs. (21b) and (21c) to obtain bosons with a well-defined 2D angular momentum. If we do so, in the symmetric phase,

$$\langle \pm 1_1|\hat{T}_\pm|0_1\rangle = \pm\sqrt{2N}, \tag{22}$$

where we denote the intrinsic ground state by $|0_1\rangle$ and the $l = \pm 1$ first excited state by $|\pm 1_1\rangle$.

Thus, the transition intensity between the first excited state and the ground state in the symmetric phase is calculated as

$$\frac{T}{N} = \frac{1}{2}\frac{|\langle 1_1|\hat{T}_+|0_1\rangle|^2 + |\langle -1_1|\hat{T}_-|0_1\rangle|^2}{N} = 2, \tag{23}$$

where the factor $\frac{1}{2}$ takes the first excited-state degeneracy into account.

The calculation of the transition intensity in the deformed region in the mean-field limit is hampered by the appearance of an infinitely degenerate band of states in the large-N limit (Goldstone modes). In particular, as the model Hamiltonian correlation energy diagram shows [19], the first excited state collapses with the ground state in the deformed phase for $\xi = 1$. As we have explained in the calculation of the $\Delta_{1\text{ph}}$ energy gap, the excitation (20c) becomes a spurious rotational degree of freedom in the deformed region. Thus, in order to correctly compute the vibrational transition intensity in this region, the excitation (20c) has to be excluded, and we only consider the physical boson $b_2^\dagger$ (20b). Therefore, in the broken-symmetry phase,

$$\frac{T}{N} = \frac{|\langle 1_1|\hat{T}_+|0_1\rangle|^2 + |\langle 1_1|\hat{T}_-|0_1\rangle|^2}{N} = 2\left(\frac{1-r^2}{1+r^2}\right)^2. \tag{24}$$

If we substitute the equilibrium value of r, $r_e = \sqrt{(5\xi-1)/(3\xi+1)}$, in Eq. (24), we obtain

$$\frac{T}{N} = \frac{(1-\xi)^2}{8\xi^2}. \tag{25}$$

As noted below, the appearance of the Goldstone modes in the broken-symmetry phase implies that, in the calculation of T/N, the initial excited state is the second $l = 1$ state $|1_2\rangle$, because the first state is a Goldstone mode. Note that Eqs. (23) and (25) are derived in the TDA approximation, and thus, they are not fully self-consistent.

Following Ref. [30], the transition to the first excited state (Goldstone boson) can be taken into consideration defining T', a new observable in the deformed region,

$$\frac{T'}{N} = \frac{|\langle 0_1|\hat{T}_+|0_1\rangle|^2 + |\langle 0_1|\hat{T}_-|0_1\rangle|^2}{N} = 8N\frac{r^2}{(1+r^2)^2}. \tag{26}$$

If we again substitute the radial coordinate equilibrium value, we obtain

$$\frac{T'}{N} = N\frac{(5\xi-1)(1+3\xi)}{8\xi^2}. \tag{27}$$

Note that this result is only valid for the broken-symmetry region where this observable is defined. As noticed in Ref. [30], T scales as N while T' scales as N^2.

We proceed to compare the obtained mean-field results with numerical calculations for a number of bosons N that is large enough to minimize finite-size effects ($N = 1000$). The numerical calculations included in the present paper have been performed using the programs in the FORTRAN package TRIAT_U3 [32].

In panels (a) and (b) of Fig. 1, we depict the ground-state energy per particle and the normalized expectation value of the u(2) number operator in the system's ground state, $\langle\hat{n}\rangle/N$, respectively. In both cases, the agreement between the numerical calculation and the mean-field result is remarkable. The second observable is considered as a quantal order parameter for the ground-state QPT: It is zero in the symmetric phase and nonzero once the critical point is crossed.

In Fig. 1(b), we also include the schematic phase diagram associated with model Hamiltonian (7). Having only one control parameter, the phase diagram is 1D, with two possible phases, symmetric (orange) and deformed (blue), also denoted as linear and bent, separated by a continuous (second-order)

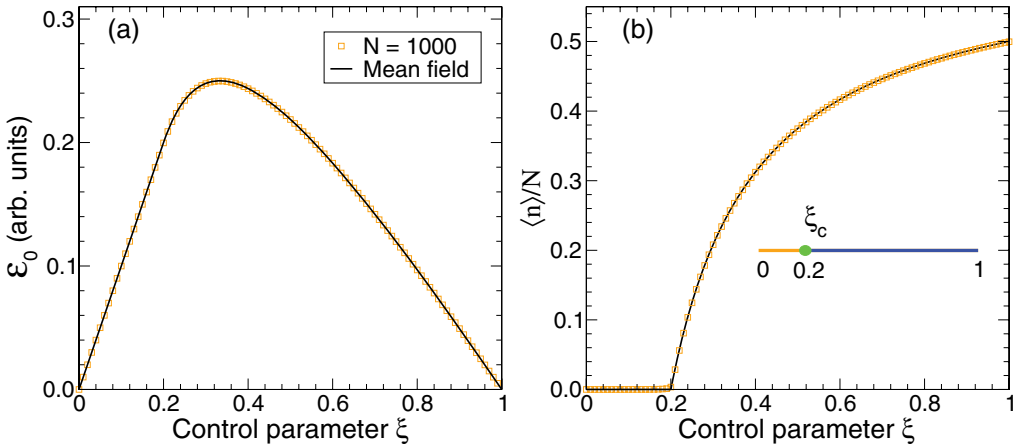

FIG. 1. (Color online) Mean-field (black line) and numerical $N = 1000$ results (orange squares) for (a) the ground-state energy per particle ($\mathcal{E}_0$) and (b) the normalized expectation value of the τ boson number operator $\hat{n}$ in the ground state ($\langle\hat{n}\rangle/N$) as a function of the control parameter ξ.

phase transition at the critical point $\xi = \xi_c = 0.2$ (green dot) [19].

The next observable considered is $\Delta_{1\mathrm{ph}}$, the energy gap between the ground state and the first excited state that is depicted in Fig. 2. In this case, as explained above, the comparison between mean-field and numerical results takes place for different states in the two phases. In the symmetric region, the comparison is performed with the numerical energy gap for the first excited state with $l = 1$ (orange squares in Fig. 2), while in the broken-symmetry region, the energy gap is computed for the second $l = 1$ excited state (red circles in Fig. 2). In both cases, there is good agreement between the analytical results close to the dynamical symmetries ($\xi = 0$ and $\xi = 1$) but, as expected, the agreement is far worse in the region around the critical point $\xi_c = 0.2$.

It is important to emphasize that, on one hand, the 1_1 excited state corresponds to a one-vibrational quantum in the symmetric phase, while in the deformed region, it belongs to the infinitely degenerate rotational band associated with the Goldstone boson. On the other hand, the 0_2 state is a two-vibrational quanta state in the symmetric phase and a one-vibrational quantum in the deformed region.

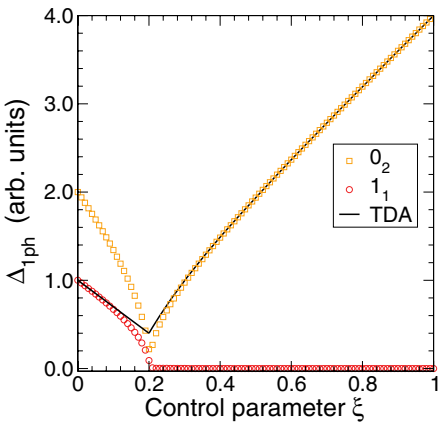

FIG. 2. (Color online) Mean-field (black line) and numerical $N = 1000$ results (orange squares and red circles) for the energy gap ($\Delta_{1\mathrm{ph}}$) as a function of the control parameter ξ.

The mean-field result for the normalized transition probability is compared with numerical results for $N = 1000$ in panels (a) and (b) of Fig. 3. In panel (a), we depict T'/N^2. This observable is defined in the deformed region, and it is compared with the numerical result for the transition of the $\pm 1_1$ to 0_1 transition. In Fig. 3(b), we compare the mean-field approximation to T, normalized by N, with numerical results. In this case, the numerical calculation is performed for the $\pm 1_1$ to 0_1 transition in the symmetric region. The $\pm 1_1$ states belong to the Goldstone band in the broken-symmetry region, therefore, we compare with numerical results for the $\pm 1_2$ to 0_1 transition in this region. We obtain good agreement between the numerical and the mean-field results that again, as expected, worsens in the vicinity of the critical region.

III. FINITE-SIZE CORRECTIONS TO THE MEAN-FIELD LIMIT

The intrinsic state analysis performed in the preceding section is exact only in the mean-field or thermodynamic limit ($N \to +\infty$). For finite N values, the mean-field results are only valid up to order N. If further corrections are sought, e.g., order N^0 effects, it is necessary to go beyond the mean-field approximation. The calculations of such analytical corrections to the mean-field limit sensitively improve the observables' description in the region around the critical value of the control parameter where mean-field approximation results badly fail. To accomplish this task, we adapt the approach used in Ref. [30] to this particular bosonic u(3) algebraic model under consideration. In this way, first, we perform a Holstein-Primakoff expansion [45] and a shift transformation, followed by a Bogoliubov transform. We first show the results for the Holstein-Primakoff expansion and the shift. In the following two subsections, we carry out the Bogoliubov transformation and extract the finite-size corrections for each geometrical phase.

The Holstein-Primakoff expansion [45] offers an expansion in powers of $1/N$ that keeps the operator Hermiticity and

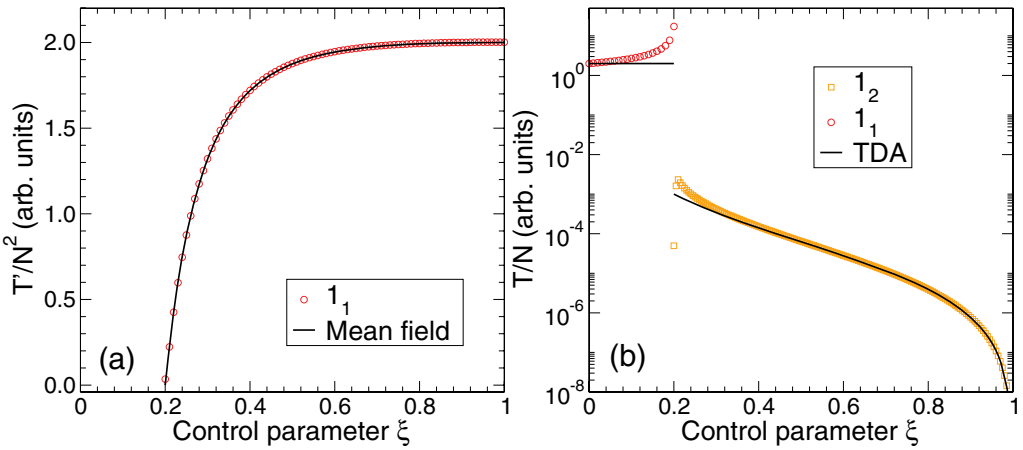

FIG. 3. (Color online) TDA (black lines) and numerical $N = 1000$ results (orange squares and red circles) for the observables T'/N^2 [panel (a)] and T/N [panel (b)] as a function of the control parameter ξ. The T' observable, depicted in panel (a), is defined only in the broken-symmetry region ($\xi > \xi_c$). The T observable in panel (b) is compared with the numerical results for the transition $\pm 1_1$ to 0_1 in the symmetric region ($\xi < \xi_c$) and the transition $\pm 1_2$ to 0_1 in the broken-symmetry region ($\xi > \xi_c$) (see text).

preserves boson commutation relations (for a review on bosonic expansion methods, see Ref. [46]). We recover the mean-field-limit result as the leading order of the expansion.

In the Holstein-Primakoff expansion, the scalar σ boson is removed by a transformation to a new set of Cartesian bosons b_i, $i = x, y$ with the usual bosonic commutation relations $[b_i, b_j^\dagger] = \delta_{ij}$. The new bosons $b_i^\dagger(b_i)$ are introduced as

$$\tau_i^\dagger \tau_j = b_i^\dagger b_j, \tag{28a}$$

$$\tau_i^\dagger \sigma = \sqrt{N}\, b_i^\dagger \sqrt{1 - \hat{n}_b/N} = (\sigma^\dagger \tau_i)^\dagger, \tag{28b}$$

$$\hat{n}_\sigma = \sigma^\dagger \sigma = N - \hat{n}_b, \tag{28c}$$

where $i, j = x, y$, and $\hat{n}_b = b_x^\dagger b_x + b_y^\dagger b_y$. The $b_i^\dagger$ bosons satisfy bosonic commutation relations at each order in N in the Taylor expansion of the square root in Eq. (28b). A third set of bosons $c_i^\dagger(c_i)$ with $i = x, y$ is defined by a shift transformation,

$$b_i^\dagger = \sqrt{N}\lambda \delta_{ix} + c_i^\dagger, \tag{29}$$

where $i = x, y$. The λ shift parameter is zero in the spherical phase and different from zero in the deformed phase.

Prior to the application of the Holstein-Primakoff expansion to the model Hamiltonian, we expand the $1/(N-1)$ factor in Eq. (7) as a series $1/(N-1) = 1/N + 1/N^2 + O(1/N^3)$. In the Holstein-Primakoff expansion, the quotient $\hat{n}_b/N$ is assumed to be small to expand the square root in a power series. When this transformation is carried out on Hamiltonian (7), the result is an expansion in powers of N with terms,

$$\hat{\mathcal{H}} = \hat{H}_1 + \hat{H}_{1/2} + \hat{H}_0 + O(1/\sqrt{N}), \tag{30}$$

where $\hat{H}_i$ incorporates the terms with a N^i dependence.

The first term is

$$\hat{H}_1 = N[\xi + (1 - 5\xi)\lambda^2 - 4\xi\lambda^4]. \tag{31}$$

Setting $\lambda = r/\sqrt{1 + r^2}$, after some trivial algebra, $\hat{H}_1$ reduces to the mean-field result (11). Equilibrium values of the order parameter and the resulting system's phase diagram are computed from the minimization of this term. In the u(3) model, we recover the phase diagram included in Fig. 1(b).

The next order in the expansion of the model Hamiltonian $\hat{H}_{1/2}$ is

$$\hat{H}_{1/2} = \sqrt{N}\lambda[1 + \xi(8\lambda^2 - 5)](c_x^\dagger + c_x). \tag{32}$$

This term goes to zero once the equilibrium values of r (or λ) are substituted. This stems from the relation $\hat{H}_{1/2} = \frac{2}{\sqrt{N}} \frac{d\hat{H}_1}{d\lambda}$. Thus, the first finite-size correction to the mean-field limit is the $\hat{H}_0$ term, which is quadratic in the c boson operators,

$$\begin{aligned} H_0 = {} & \lambda^2(4\lambda^2 - 1)\xi + (1 - 3\xi + 14\lambda^2\xi)c_x^\dagger c_x \\ & + (1 - 3\xi + 4\lambda^2\xi)c_y^\dagger c_y + (5\lambda^2 - 1)\xi(c_x^\dagger c_x^\dagger + c_x c_x) \\ & + (2\lambda^2 - 1)\xi(c_y^\dagger c_y^\dagger + c_y c_y). \end{aligned} \tag{33}$$

We proceed detailing how this contribution is brought to diagonal form by a Bogoliubov transformation in the symmetric and deformed phases. The obtained analytical results are compared to the results of numerical diagonalization of the model Hamiltonian for finite-N values in the next section.

A. Symmetric phase

The symmetric case, which is also known as the linear configuration in molecular structure, is obtained for control parameter values $0 \leqslant \xi \leqslant 0.2$. The associated order parameter is $r_e = 0$ and, consequently, $\lambda_e = 0$. The resulting H_0 has the same dependence for x and y,

$$H_{0,\mathrm{sym}} = \Theta \sum_{i=x,y} c_i^\dagger c_i + \Delta \sum_{i=x,y} (c_i^\dagger c_i^\dagger + c_i c_i), \tag{34}$$

with $\Theta = 1 - 3\xi$ and $\Delta = -\xi$. The Hamiltonian (34) can be diagonalized with a Bogoliubov transformation,

$$\begin{aligned} c_i^\dagger &= u_i a_i^\dagger + v_i a_i, \\ c_i &= u_i a_i + v_i a_i^\dagger, \end{aligned} \tag{35}$$

where $i = x, y$. If we impose that the transformation is canonical and that nondiagonal terms in the a bosons vanish after the transformation, we obtain the set of equations,

$$\begin{aligned} \Delta(u^2 + v^2) + \Theta uv = 0, \\ u^2 - v^2 = 1, \end{aligned} \tag{36}$$

where we have removed the subindex i because the transformation is common to the x and y degrees of freedom. The solution of Eqs. (36) is

$$\begin{aligned} u &= \sqrt{\frac{1}{2}\left(1 + \frac{\Theta}{\sqrt{\Theta^2 - 4\Delta^2}}\right)}, \\ v &= -\sqrt{\frac{1}{2}\left(-1 + \frac{\Theta}{\sqrt{\Theta^2 - 4\Delta^2}}\right)}. \end{aligned} \tag{37}$$

Once the Bogoliubov transformation is performed, the Hamiltonian (34) is brought to diagonal form

$$H_{0,\mathrm{sym}} = [3\xi - 1 + \Xi^{\mathrm{sym}}(\xi)^{1/2}] + \Xi^{\mathrm{sym}}(\xi)^{1/2}\hat{n}_a + O(1/N), \tag{38}$$

where $\hat{n}_a$ is the number operator for a bosons and $\Xi^{\mathrm{sym}} = (1 - 5\xi)(1 - \xi)$.

When we consider the mean-field result (12) and the computed N^0 correction (38), the resulting ground-state energy per particle and first excited-state energy gap are

$$\mathcal{E}_0^{\mathrm{sym}} = \xi + N^{-1}[3\xi - 1 + \Xi^{\mathrm{sym}}(\xi)^{1/2}], \tag{39a}$$

$$\Delta_{1\mathrm{ph}}^{\mathrm{sym}} = \Xi^{\mathrm{sym}}(\xi)^{1/2}. \tag{39b}$$

We can also easily calculate the correction to the expected value of the number of τ bosons in the ground state, taking advantage of the Hellman-Feynman theorem: The derivative of the eigenvalue of a given operator is equal to the expectation value of the derivative of this operator with the corresponding eigenfunction. If we define a new control parameter x such that $\xi = \frac{1}{1+x}$, applying the Hellman-Feynman theorem and taking into account that the mean-field component for this observable vanishes, we obtain

$$\begin{aligned} \frac{\langle \hat{n} \rangle}{N} &= \frac{d}{dx}\left[(1 + x)\mathcal{E}_0^{\mathrm{sym}}(x)\right] \\ &= \frac{1}{N}\frac{1 - 3\xi - \Xi^{\mathrm{sym}}(\xi)^{1/2}}{\Xi^{\mathrm{sym}}(\xi)^{1/2}} + O(N^{-2}). \end{aligned} \tag{40}$$

The last observable considered is T, the transition probability between the ground state and the first excited state. The starting point to obtain BMF results for the matrix elements of the transition intensity operator (18) is its expression in terms of Cartesian bosons and the application of the Holstein-Primakoff expansion (28) and the shift transformation (29). The obtained expression for $\hat{T}_\pm$, fixing $\lambda = 0$, is

$$\begin{aligned} \hat{T}_\pm = -\sqrt{N}\{&(c_x^\dagger + c_x) \pm i(c_y^\dagger + c_y) \\ &+ \frac{1}{2N}[c_x^\dagger \hat{n}_c + \hat{n}_c c_x + i(c_y^\dagger \hat{n}_c + \hat{n}_c c_y)]\}. \end{aligned} \tag{41}$$

If we substitute the c bosons with the a bosons via the Bogoliubov transformation defined in Eqs. (35) and (36) and we take into account that the first excited state is doubly degenerate $|\pm 1_1\rangle = \mp\frac{a_x^\dagger \pm i a_y^\dagger}{\sqrt{2}}|0\rangle$, we obtain the following result:

$$\langle \pm 1_1 | \hat{T}_\pm | 0_1 \rangle = \mp\sqrt{2N}(u + v). \tag{42}$$

In this case, the observable T is

$$\frac{T}{N} = \frac{|\langle 1_1|\hat{T}_+|0_1\rangle|^2 + |\langle -1_1|\hat{T}_-|0_1\rangle|^2}{2N} = 2\sqrt{\frac{1 - \xi}{1 - 5\xi}}. \tag{43}$$

This result coincides with the first-order term in the expansion of the observable T in Ref. [30], and it permits the calculation of the scaling exponent associated with this observable. However, it does not coincide with the TDA result (23). The next correction (order zero in N) cannot be computed at this level and implies a more elaborate Bogoliubov transformation, including terms of a higher order than linear in the creation and annihilation operators [47].

B. Deformed phase

The deformed phase, which is known as the bent phase in molecular structure, is obtained for the control parameter interval $0.2 < \xi \leqslant 1$. The associated order parameter is $r_e = \sqrt{\frac{5\xi - 1}{3\xi + 1}}$ and, consequently, $\lambda_e^2 = \frac{5\xi - 1}{8\xi}$. In this case, the resulting H_0 has a different dependence in x and y,

$$H_{0,\mathrm{def}} = \lambda^2(4\lambda^2 - 1)\xi + \sum_{i=x,y} \Theta_i c_i^\dagger c_i + \sum_{i=x,y} \Delta_i (c_i^\dagger c_i^\dagger + c_i c_i), \tag{44}$$

with

$$\begin{aligned} \Theta_x &= 1 + (14\lambda^2 - 3)\xi, \\ \Theta_y &= 1 + (4\lambda^2 - 3)\xi, \\ \Delta_x &= (5\lambda^2 - 1)\xi, \\ \Delta_y &= (2\lambda^2 - 1)\xi. \end{aligned}$$

We apply a Bogoliubov transformation to Eq. (44) and follow the procedure defined in the symmetric case. In this case, the solution (37) is valid, although the x and y components have to be treated separately. We obtain

$$H_{0,\mathrm{def}} = E_0^{\mathrm{def}} + \frac{\Xi_x(\xi)^{1/2}}{2}\hat{n}_{a_x} + \frac{\Xi_y(\xi)^{1/2}}{2}\hat{n}_{a_y} + O(1/N), \tag{45}$$

where $\hat{n}_{a_i}$ is the number operator for the a_i bosons with $i = x, y$ and

$$E_0^{\mathrm{def}} = (3 - 10\lambda^2 + 4\lambda^4)\xi - 1 + \Xi_x(\xi)^{1/2} + \Xi_y(\xi)^{1/2}, \tag{46}$$

$$\Xi_x(\xi) = 1 + (28\lambda^2 - 6)\xi + (5 - 44\lambda^2 + 96\lambda^4)\xi^2, \tag{47}$$

$$\Xi_y(\xi) = 1 + (8\lambda^2 - 6)\xi + (5 - 8\lambda^2)\xi^2. \tag{48}$$

The ground-state energy per boson and the first excited-state energy gap are computed considering this correction with $\lambda_e^2 = \frac{5\xi - 1}{8\xi}$ and the zero energy mean-field result from Eq. (12),

$$\begin{aligned} \mathcal{E}_0^{\mathrm{def}} = &\frac{-9\xi^2 + 10\xi - 1}{16\xi} \\ &+ N^{-1}\left[\frac{1 - 6\xi - 27\xi^2 + 8\xi\,\Xi^{\mathrm{def}}(\xi)^{1/2}}{16\xi}\right], \end{aligned} \tag{49a}$$

$$\Delta_{1ph}^{\mathrm{def}} = \Xi^{\mathrm{def}}(\xi)^{1/2}, \tag{49b}$$

where $\Xi^{\rm def}(\xi)=\Xi_x(\xi)=(5\xi-1)(1+3\xi)$. The y-coordinate contribution is a spurious Goldstone boson, associated with a ground-state rotation.

As in the symmetric case, we calculate the correction to the expected value of the number of τ bosons in the ground state making use of the Hellman-Feynman theorem and the change in variable $\xi=\frac{1}{1+x}$,

$$\frac{\langle\hat{n}\rangle}{N}=\frac{\Xi^{\rm def}(\xi)}{8\xi(1+3\xi)}+\frac{1}{N}\frac{4\xi(\xi-1)+(1-3\xi)\Xi^{\rm def}(\xi)^{1/2}}{8\xi\,\Xi^{\rm def}(\xi)^{1/2}}+O(N^{-2}). \tag{50}$$

The last observable considered is the transition probability between the ground state and the first excited state. In this case, as explained in the mean-field case, we distinguish between the T and T' observables.

Taking into account that the y degree of freedom is spurious, the BMF expansion in the deformed phase of the transition operator is

$$\begin{aligned}\hat{T}_\pm=&-\sqrt{N}\sqrt{1-\lambda^2}\\&-\left\{2\lambda\sqrt{N}\left[1-\frac{1}{2\sqrt{N}}\frac{\lambda}{1-\lambda^2}(c_x^\dagger+c_x)-\frac{1}{2N}\frac{1}{1-\lambda^2}\hat{n}_c\right]\right.\\&+c_x^\dagger\left[1-\frac{1}{2\sqrt{N}}\frac{\lambda}{1-\lambda^2}(c_x^\dagger+c_x)-\frac{1}{2N}\frac{1}{1-\lambda^2}\hat{n}_c\right]\\&\left.+\left[1-\frac{1}{2\sqrt{N}}\frac{\lambda}{1-\lambda^2}(c_x^\dagger+c_x)-\frac{1}{2N}\frac{1}{1-\lambda^2}\hat{n}_c\right]c_x\right\},\end{aligned} \tag{51}$$

with Bogoliubov coefficients,

$$u_x=\frac{1}{\sqrt{2}}\sqrt{1+\frac{23\xi-3}{4\sqrt{(5\xi-1)(3\xi+1)}}}, \tag{52}$$

$$v_x=-\frac{1}{\sqrt{2}}\sqrt{-1+\frac{23\xi-3}{4\sqrt{(5\xi-1)(3\xi+1)}}}. \tag{53}$$

We substitute the c bosons with the a bosons via the Bogoliubov transformation defined in Eq. (35), and we take into account that, in this case, the first excited state is $|1_1\rangle=a_x^\dagger|0_1\rangle$. Doing so, we obtain that the matrix element of the transition operator in the broken-symmetry phase is

$$\begin{aligned}\langle 1_1|\hat{T}_\pm|0_1\rangle=&-\sqrt{N}\sqrt{1-\lambda^2}\langle 0_1|a_x\\&\times\left[2\lambda\sqrt{N}+\frac{1-2\lambda^2}{1-\lambda^2}(u_x+v_x)(a_x^\dagger+a_x)\right]|0_1\rangle\\=&-\sqrt{N}\frac{1-2\lambda^2}{\sqrt{1-\lambda^2}}(u_x+v_x).\end{aligned} \tag{54}$$

As in the symmetric phase, the corrections that have a lower order in N cannot be extracted without applying a more general Bogoliubov approach. Up to the present order, the observable T is

$$\begin{aligned}\frac{T}{N}=&\frac{|\langle 1_1|\hat{T}_+|0_1\rangle|^2+|\langle 1_1|\hat{T}_-|0_1\rangle|^2}{2N}=\frac{(1-2\lambda^2)^2}{1-\lambda^2}(u_x+v_x)^2\\=&\frac{(\xi-1)^2}{4\xi\sqrt{(5\xi-1)(1+3\xi)}}.\end{aligned} \tag{55}$$

In the T' case, the relevant expectation value of the transition operators (51) is

$$\begin{aligned}\frac{T'}{N}=&\frac{|\langle 0_1|\hat{T}_+|0_1\rangle|^2+|\langle 0_1|\hat{T}_-|0_1\rangle|^2}{N}=8\lambda^2(1-\lambda^2)\\=&\frac{(1+3\xi)(5\xi-1)}{8\xi^2}N,\end{aligned} \tag{56}$$

where we recover the result calculated in the mean-field limit. As in the previous case, we cannot go beyond this result with the Bogoliubov transformation (35).

IV. COMPARISON WITH NUMERICAL RESULTS

The algebraic Hamiltonian (7) can be diagonalized numerically once an appropriate basis is defined. In the present section, we compare the numerical, the mean-field, and the beyond mean-field (BMF) analytical corrections. To carry out the numerical diagonalization, we use the basis associated with dynamical symmetry I [16,19]. The results obtained for the four observables under study are the following.

A. Ground-state energy per particle

In Fig. 4, we depict the results obtained for this observable using the above-mentioned different approaches. The thin dashed black line is the (N-independent) mean-field result given in Eq. (12); red circles denote the results after numerical diagonalization of the model Hamiltonian for $N=40$. The finite-N correction to the symmetric phase $0\leqslant\xi\leqslant 0.2$, given in Eq. (39a), is depicted with a thick orange line. The deformed phase correction (49a), valid for control parameter values $0.2<\xi_c\leqslant 1$, is indicated by a thick blue line.

It is apparent that mean-field results and computed corrections are both good approximations for control parameter values close to a dynamical symmetry (ξ values close to 0 or 1). However, the agreement, when the finite-N corrections are considered, is far better than the pure mean-field approach as the control parameter takes values closer to the critical value

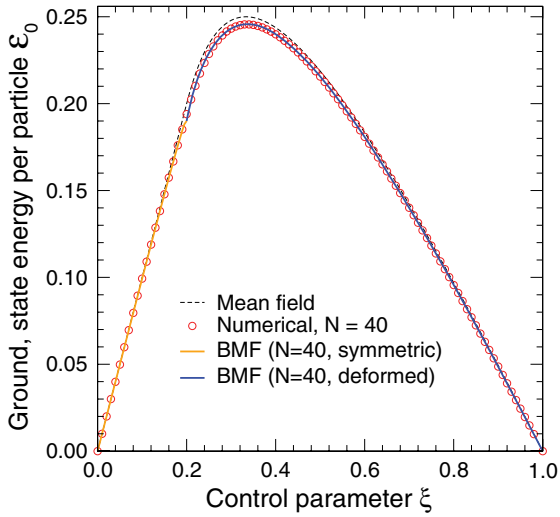

FIG. 4. (Color online) Ground-state energy per particle of Hamiltonian (7) in arbitrary units as a function of the control parameter ξ, $\mathcal{E}_0(\xi)$, in various approximations (see text).

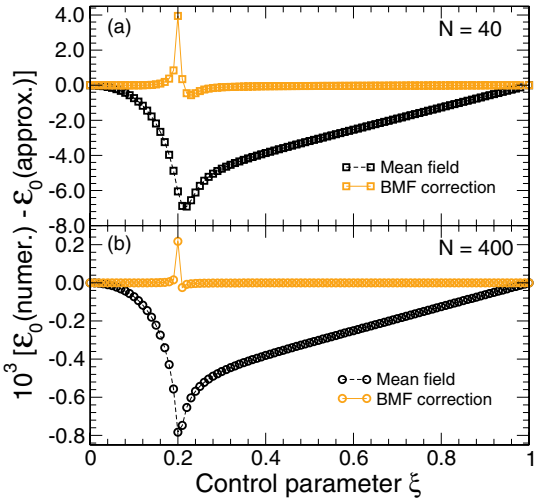

FIG. 5. (Color online) Difference between the ground-state energy per particle obtained numerically and using the two analytical approximations considered in this paper. Panel (a) displays the results obtained for $N = 40$, and panel (b) displays the results obtained for $N = 400$ as a function of the control parameter.

$\xi_c = 0.2$. At the precise critical value $\xi = 0.2$, the corrections display a kink that is characteristic of this approach.

The difference between the numerical and the BMF results at this scale is difficult to discern. To clarify the improvement obtained including the BMF correction, in Fig. 5, we depict the difference between numerical results and mean-field and corrected mean-field results for $N = 40$ and 400. As expected, both analytical approximations improve as N increases and, in both cases, the derived BMF correction is much closer (to order $1/N$) to the numerical diagonalization. These differences between numerical and analytical approximations follow a similar pattern as the results presented in Ref. [30].

As shown in Fig. 5, the computed analytical correction to the ground-state energy per particle clearly improves mean-field results. The difference between numerical and analytical approaches is far smaller in the BMF case (full orange line), and it only gets appreciable in a very small region around the critical point.

B. First excited-state energy gap

The numerical results for this observable are depicted in Fig. 6, together with the mean-field result and the BMF correction for the symmetric and deformed phases. The numerical results for $N = 40$ are represented as orange circles for the 0_2-state energy gap and as green squares for the 1_1-state energy gap. The dashed black line is the TDA result (17b). The analytical corrections to the mean-field approach in the symmetric (39b) and deformed (49b) phases are depicted using thick orange and blue lines, respectively.

As previously stated, when the critical point is crossed, the first intrinsic excitation in the symmetric region (1_1 state, green squares in Fig. 6) becomes a Goldstone boson in the broken phase, where the first intrinsic excitation corresponds to a two-quanta state in the symmetric region (0_2 state, orange circles in Fig. 6). This is in good agreement with the results published in Ref. [30] for u($2L + 1$)-so($2L + 2$) transitions.

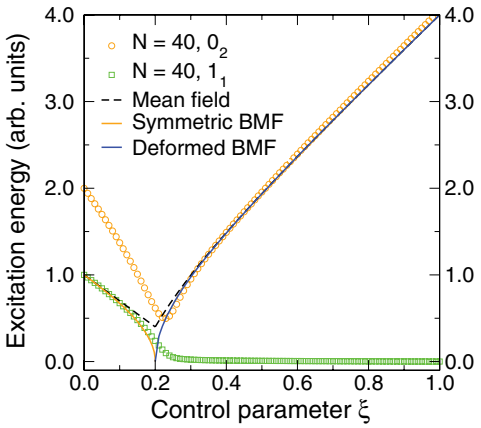

FIG. 6. (Color online) Energy gap ($\Delta_{1\text{ph}}$) for the Hamiltonian (7) as a function of the control parameter ξ. Numerical $N = 40$ results for 0_2 and 1_1 states are shown as (orange) circles and (green) squares.

As in the previous case, the new analytical expression for the energy gap clearly improves TDA results and adequately describes numerical results up to values of the control parameter closer to the critical point.

C. Expectation value of the number operator

Numerical and analytical results for the expectation value in the system's ground state of the u(2) number operator $\hat{n}$ are depicted in Fig. 7. In Fig. 7(a), we show the behavior for the full range of values of the control parameter. A zoom of the region around the critical value is presented in panel (b) of this figure. In both panels, numerical results for $N = 40$ are represented with red circles; the thin dashed black line is the normalized mean-field result (13), and the analytical correction to the mean-field approach in the symmetric (40) and deformed (50) phases is depicted using thick orange and blue lines, respectively.

As expected, the accordance between analytical and numerical results is remarkably better in the case of the BMF approximation for both phases, symmetric and deformed. As for the previous observables, the discrepancy with numerical results diminishes for increasing values of N. In the vicinity of the critical point, the computed corrections (40) and (50) become singular. This divergence can be corrected by computing more terms in the $1/N$ expansion (30). This has already been performed for other bosonic two-level systems using the continuous unitary transformations (CUTS) approach [30,48–51]. The divergent behavior is useful in the calculation of finite-size critical exponents, as shown in the next section.

D. Transition probability

The comparison of the different analytical results for T/N with a numerical calculation for $N = 40$ can be found in Fig. 8. In panel (a) of this figure, the TDA calculation (broken line) and the present paper's result (43) are compared with numerical results for $N = 40$ (red circles). The numerical results are computed for the transition of the first excited state $\pm 1_1$ to the ground state.

The results for the observable T in the broken-symmetry region are shown in panel (b) of Fig. 8. In this case, the first

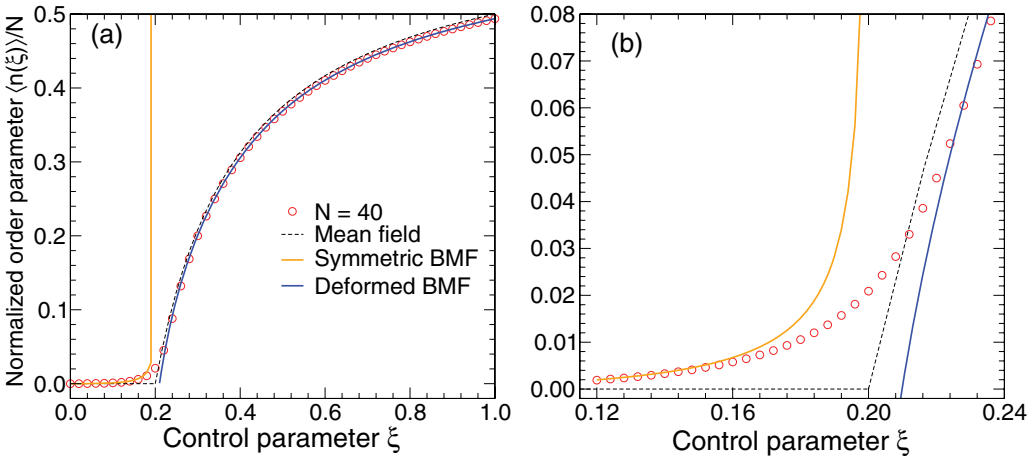

FIG. 7. (Color online) Normalized expectation value of the u(2) number of bosons ($\hat{n}$) in the ground state of the Hamiltonian (7) as a function of the control parameter ξ. Numerical ($N = 40$) results are depicted with (red) circles, mean-field calculations are depicted with a thin dashed black line, and BMF results are depicted in the symmetric and deformed phases as thick orange and blue lines (see text). Panel (b) is a zoom of the region around the critical value of the control parameter.

excited state with $l = 1$ is a Goldstone mode, and the numerical results are computed for the second $l = 1$ excited state 1_2 and again for $N = 40$.

The mean-field result for T' in the deformed region (56) is depicted in Fig. 9, comparing the analytical results with a numerical calculation for $N = 40$.

The analytical result for T in the symmetric region (43) greatly improves the agreement obtained with the TDA calculation. In the case of T', the BMF correction cannot be calculated with the levels of theory used in the present paper, and its inclusion demands a nonlinear Bogoliubov transformation.

V. SCALING PROPERTIES OF THE BOSONIC u(3) APPROACH

Finite-size scaling in condensed-matter systems is a topic of major interest and has solid foundations since the formulation of a general theory [52,53] (for a review, see Ref. [54]). More recently, in the fields of nuclear and molecular structure, driven by the suggestion of a simple scale-invariant behavior for the excitation energies of nuclei at the critical point of shape-phase transitions [55–58], several groups of researchers initiated a study of finite-size scaling behavior within the context of algebraic models, paying special attention to the second-order QPT between the spherical and γ-unstable deformed phases of the IBM u(6) Hamiltonian [30,31,48,59].

We now proceed to analytically derive finite-size scaling exponents for the observables under study in the 2D limit of the vibron model. The obtained exponent values are compared to the numerical results published in Ref. [19]. Finite-size scaling exponents for a u($2L$)-so($2L + 1$) transition with semi-integer values of L ($L = 1/2$) are calculated analytically.

We obtain the scaling exponents from the derived corrections to the mean-field limit of the u(3) algebraic model

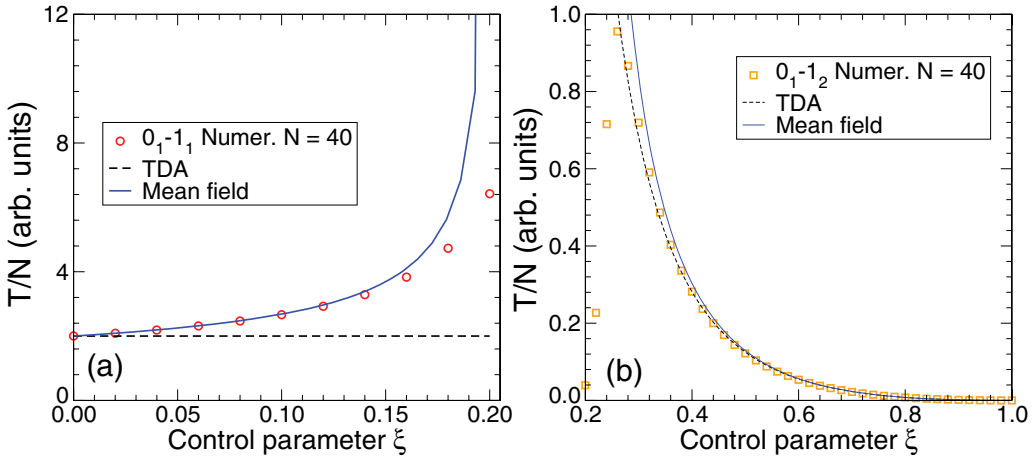

FIG. 8. (Color online) Different analytical approximations for the T observable in the symmetric [panel (a)] and deformed regions [panel (b)]. Note that, in the symmetric region, we compare with numerical results for the 1_1 state, while in the deformed sector, we compare with the transition to the 1_2 excited state (see text). TDA (broken lines) and BMF (full blue lines) results are compared to a numerical calculation (red circles and orange squares) for $N = 40$.

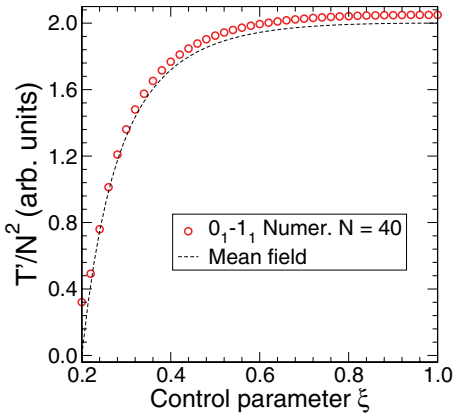

FIG. 9. (Color online) Analytical approximation to the T' observable in the broken-symmetry region. The mean field (broken line) is compared to a numerical calculation (red circles) for $N = 40$.

making use of an algorithm that profits from the singular behavior of the observable under study in the QPT critical point [30,48–51]. The critical behavior may not be apparent at the obtained correction order (e.g., ground-state energy), emerging only once subleading corrections are taken into consideration.

We make use of the extension of the Fisher and Barber results [52] to infinitely coordinated systems performed by Botet *et al.* [53] and Botet and Jullien [60]. An infinitely coordinated system is composed of N elements, each of which is coupled to all the others. It is conjectured that, for such systems, the dependence on the temperature of any observable in the vicinity of the critical point (T_c) is

$$A \sim (T - T_c)^a. \tag{57}$$

This scaling hypothesis can be extended to the case of large, but finite, N values,

$$A \sim (T - T_c)^a F_A[N(T - T_c)^\nu], \tag{58}$$

where $F_A(x) \to$ constant as $x \to \infty$ and behaves as $F_A(x) \sim x^{\omega_a}$ for $x \to 0$. This function guarantees the right behavior of the observable in the thermodynamic limit as well as a regular conduct near the critical point for finite values of N just imposing $\omega_a = -a/\nu$.

The scaling hypothesis (58) can be extended to the study of QPTs, where a Hamiltonian control parameter plays the role of the temperature, assuming that the critical behavior of any observable should be regular for finite N. In general, one can find that the $1/N$ expansion of a physical quantity $\Phi_N(\xi)$, near the critical point of the QPT, can be decomposed in a regular and a singular part as follows:

$$\Phi_N(\xi) = \Phi_N^{\rm reg}(\xi) + \Phi_N^{\rm sing}(\xi), \tag{59}$$

where $\Phi_N^{\rm sing}(\xi)$ (or its derivatives) diverges when ξ tends to ξ_c, while $\Phi_N^{\rm reg}(\xi)$ and its derivatives stay regular. The extension of the *ansatz* (58) to QPTs results in

$$\Phi_N^{\rm sing}(\xi) \simeq \frac{\Xi(\xi)^{x_\Phi}}{N^{n_\Phi}} \mathcal{F}_\Phi[N\,\Xi(\xi)^\nu], \tag{60}$$

where $\mathcal{F}_\Phi$ is a function depending only on the scaling variable $N\,\Xi(\xi)^\nu$ and $\Xi(\xi)$ includes a factor $\xi - \xi_c$ [50]. Once this functional form of $\Phi_N^{\rm sing}(\xi)$ is accepted, the scaling exponents can be obtained because, for finite-N values, physical quantities do not diverge, and, thus, $\mathcal{F}_\Phi(x) \sim x^{-x_\Phi/\nu}$, and the system's size dependence at the critical point is $\Phi_N^{\rm sing}(\xi_c) \sim N^{-n_\Phi - x_\Phi/\nu}$. Note that the term N^{-n_Φ} is explicitly included to extend the formalism for observables that are implicitly divided by a power of N.

The value of ν can be obtained from a $1/N$ expansion of the singular part of the observables under study, identifying the scaling variable in the expansion, i.e., $N\,\Xi(\xi)^\nu$. This has been performed for different systems [u(2L + 1) models] and observables (ground-state energy, gap, spin components, etc.) [30,48,50,51]. In all these cases, $\nu = 3/2$, which implies a system's size dependence $\Phi_N^{\rm sing}(\xi_c) \sim N^{-n_\Phi - 2x_\Phi/3}$.

Note that, in the present paper, the value of ν cannot be deduced in this fashion because only one term is obtained in the expansion of the singular part of each observable. However, following an argument similar to the one in Ref. [50], the obtained result for the expected number of τ bosons in the deformed region in Eq. (50) can be written in the vicinity of the critical point as

$$\frac{\langle \hat{n} \rangle}{N} \sim \frac{\Xi^{\rm def}(\xi)}{8\xi(1 + 3\xi)} + \frac{1}{N} \frac{\xi - 1}{2\Xi^{\rm def}(\xi)^{1/2}}, \tag{61}$$

where we have only considered the diverging contribution in the order $1/N$. The difference of the exponents that affect $\Xi^{\rm def}(\xi)$—i.e., $(\xi - \xi_c)$—in Eq. (61) is $1 - (-\frac{1}{2}) = \frac{3}{2}$. In the case of N, this difference is $0 - (-1) = 1$. This is in accordance with the definition of $N\,\Xi(\xi)^{3/2}$ as the system's scaling variable. The goodness of this definition is further confirmed by the agreement of the analytically computed finite-size scaling exponents with the numerical results included at the end of the present section as well as in Ref. [19].

Taking the arguments explained above into consideration, the finite-size scaling exponents can easily be calculated for the set of observables under study. If we consider, for example, the ground-state energy in the symmetric phase (39a), the regular and singular components are $\mathcal{E}_0^{\rm reg} = \xi + (3\xi - 1)/N$ and $\mathcal{E}_0^{\rm sing} = \Xi^{\rm sym}(\xi)^{1/2}/N$. Thus, $x_\Phi = 1/2$, $n_\Phi = 1$, and the scaling exponent is $N^{-4/3}$. An identical exponent is found in the deformed phase, using Eq. (49a) as a starting point. The scaling exponent values for the observables studied in this paper can be found in the third column of Table I. The obtained results coincide with the scaling exponents obtained

TABLE I. Scaling exponents for the observables under study: ground-state energy ($\mathcal{E}_0$), energy gap ($\Delta_{\rm 1ph}$), expected number of τ bosons ($\langle \hat{n} \rangle$), and the transition probability T/N.

Φ	x_Φ	n_Φ	Scaling exponent	Numerical results [19]
$\mathcal{E}_0$	+1/2	+1	−4/3	$-A_{\epsilon 1} = -0.9564(5)$[a]
$\Delta_{\rm 1ph}$	+1/2	0	−1/3	$-A_{\Gamma_{\rm 1,vib}} = -0.337\,43(10)$
$\langle \hat{n} \rangle$	−1/2	0	+1/3	$-A_{n1} + 1 = 0.3770(5)$
T/N	−1/2	0	+1/3	$0.320\,26(13)$[b]

[a]The difference, in this case, is explained by the inclusion of the regular part in the computation of the scaling exponent in Ref. [19]. See discussion in text.

[b]This scaling exponent was not computed in Ref. [19]. See discussion in text.

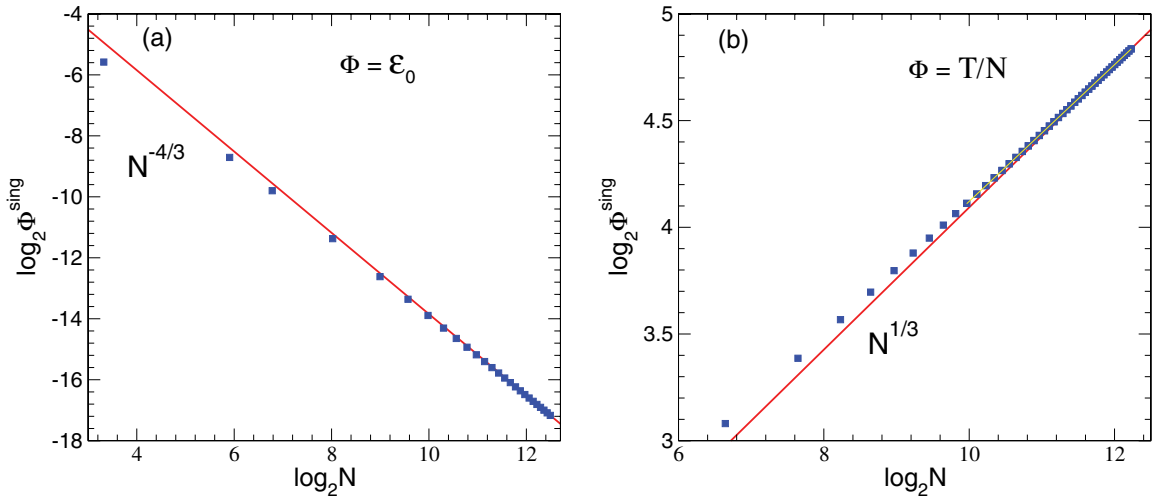

FIG. 10. (Color online) Log-log plot of the singular part of the ground-state energy per particle [$\Phi = \mathcal{E}_0$, panel (a)] and the singular part of the transition probability between the ground state and the first excited state [$\Phi = T/N$, panel (b)] evaluated at the critical control parameter ($\xi_c = 0.2$) as a function of the system's size. Both quantities are expressed in arbitrary units. Numerical results are plotted as blue squares, and the red line shows the expected power dependence.

in Ref. [30] for u(2L)-so(2L + 1) transitions with integer L values, something expected from the relation between both works pointed out in the Appendix.

The obtained scaling exponents for $\Delta_{1\mathrm{ph}}$ and $\langle \hat{n} \rangle$ agree with the numerically computed exponents from Ref. [19], as shown in the last column of Table I, and also coincide with the asymptotic values suggested in this reference. In the cases where it has been possible to estimate the asymptotic scaling exponent to the right and to the left of the critical point, both values coincide.

Because the observables' definition in the present paper and in Ref. [19] is not fully equivalent, the mapping between exponents is not always direct. To facilitate the comparison, we have included, in the last column of Table I, not only the numerical value, but also the notation for the exponent used in Ref. [19].

The difference between our result and the Ref. [19] result in the case of the ground-state scaling exponent stems from the lack of distinction between regular and singular components of this physical observable in the latter case. It can easily be seen from Eq. (39a) that, if the singular component of the ground-state energy is not isolated, the expected finite-size scaling exponent is -1 as reported in Ref. [19]. We have performed numerical ground-state energy calculations, leaving aside the regular part. The obtained results are plotted in a log-log scale in Fig. 10(a), where it can clearly be noticed that the expected dependence is well reproduced.

The transition intensity scaling exponent was not numerically estimated in Ref. [19]. Thus, we have carried out the necessary numerical calculations to check the predicted value of 1/3. Results are depicted in the log-log plot of Fig. 10(b), which makes apparent that the numerical results follow the predicted dependence with the system's size. The fit of the numerical results for $N > 1000$ gives, as a result, the scaling exponents estimation in Table I, which reasonably agrees with the theoretically predicted value.

VI. SUMMARY AND CONCLUDING REMARKS

In this paper, we have investigated the u(2)-so(3) phase transition that occurs in the u(3) algebraic approach to 2D systems. In a previous paper [19], this transition was investigated numerically, and the scaling behavior with the system size of several relevant quantities was extracted. However, obtaining the finite-size corrections from numerical studies is always a difficult task. In this paper, we have combined the Holstein-Primakoff expansion with a Bogoliubov transformation in order to analyze both phases, symmetric and nonsymmetric, of the system so as to analytically obtain the finite-size corrections for the selected observables. The analytical results obtained are valid in an interval much closer to the critical point than mean-field results and largely improve the model description.

Similar studies for cases described by a spectrum-generating algebra u(2L + 2) with $L = 0, 1, 2, \ldots$ were already presented in Ref. [30]. However, the present case, which is the simplest with a half-integer value of L [u(3) corresponds to $L = 1/2$] is studied here. The analytical results for the observables discussed (the ground-state energy, the gap, the expectation value of the boson number in the upper level that is considered the quantal order parameter for the transition, and the reduced transition probability between the first excited and the ground states) provide specific finite-size corrections for all the observables studied. The results for the finite-size corrections numerically obtained in Ref. [19] are consistent, after reinterpretation of the calculations in some cases, with the analytical results presented here.

ACKNOWLEDGMENTS

This work has been partially supported by the Spanish MEC, by the European regional development fund (FEDER) under Projects No. FIS2008-04189 and CPAN-Ingenio (No. CSD2007-00042), and by the Junta de Andalucía (Projects No. P07-FQM-02962, No. P07-FQM-03014, and

No. P07-FQM-02894). P.P.F. acknowledges the Spanish MEC for an FPU grant. The authors thank Jorge Dukelsky, Francesco Iachello, Pieter van Isacker, Amiram Leviatan, and Armando Relaño for valuable comments and suggestions.

APPENDIX: RELATION WITH RESULTS OBTAINED USING CUTS

In Ref. [30], the case of QPTs in two-level boson systems, the lowest level with zero angular momentum and the upper one with integer angular momentum L, was analyzed. These systems have a spectrum-generating algebra u$(2L+2)$ and present dynamical symmetries u$(2L+1)$ and so$(2L+2)$, both having a common so$(2L+1)$ symmetry. Reference [30] explored the u$(2L+1)$ to so$(2L+2)$ transition in these systems, and the corresponding finite-size corrections for different observables were obtained using the CUTS method. For that purpose, the boson-pairing Hamiltonian was used

$$\begin{aligned} H' &= xn_L + \frac{1-x}{(N-1)}\hat{P}' \\ &= xn_L + \frac{1-x}{4(N-1)}(P_L^\dagger P_L + P_s^\dagger P_s - P_L^\dagger P_s - P_s^\dagger P_L), \end{aligned} \tag{A1}$$

where $\hat{P}'$ is the pairing operator used, which is related to the so$(2L+2)$ Casimir operator, defined as

$$\hat{P}' = \tfrac{1}{4}(P_L^\dagger - P_s^\dagger)(P_L - P_s), \tag{A2}$$

with

$$n_L = \sum_{\mu=-L}^{+L} L_\mu^\dagger L_\mu, \tag{A3}$$

$$P_s^\dagger = (P_s)^\dagger = s^\dagger s^\dagger, \tag{A4}$$

$$P_L^\dagger = (P_L)^\dagger = \sum_{\mu=-L}^{+L} (-1)^\mu L_\mu^\dagger L_{-\mu}^\dagger = L^\dagger L^\dagger. \tag{A5}$$

$L_\mu^\dagger$ creates a boson in the excited L level with projection μ, while L_μ destroys it. The total number of bosons $N = n_s + n_L$ is a conserved quantity. All systems cited and worked out in that paper had L integer values: $L=0$ corresponds to the Lipkin model, $L=1$ is the molecular vibron model, $L=2$ is the nuclear interacting boson model, etc. One can realize that the finite-size corrections obtained for the present u(3) model are identical to those obtained with the formalism presented in Ref. [30] if a half-integer $L=1/2$ angular momentum for the upper level is selected and an appropriate change in the control parameter is made. In this appendix, we would like to show that the Hamiltonian (A1) can be rewritten as the u(3) Hamiltonian (7) and that the results presented in Ref. [30] can also be used for the L half-integer.

In our case, the Hamiltonian reads

$$\hat{\mathcal{H}} = \varepsilon\left[(1-\xi)\hat{n} + \frac{\xi}{N-1}\hat{P}\right]. \tag{A6}$$

With the definitions of $\hat{P}$, Eqs. (5) and (6), and defining

$$n_\sigma = \sigma^\dagger\sigma, \tag{A7}$$

$$n_\tau = \tau_+^\dagger\tau_+ + \tau_-^\dagger\tau_-, \tag{A8}$$

$$P_\sigma^\dagger = (P_\sigma)^\dagger = \sigma^\dagger\sigma^\dagger, \tag{A9}$$

$$P_\tau^\dagger = (P_\tau)^\dagger = \tau^\dagger\tau^\dagger = 2\tau_+^\dagger\tau_-^\dagger, \tag{A10}$$

after some algebra, the so(3) pairing operator $\hat{P}$ (6) can be written as

$$\hat{P} = (P_\tau^\dagger P_\tau + P_\sigma^\dagger P_\sigma + P_\tau^\dagger P_\sigma + P_\sigma^\dagger P_\tau), \tag{A11}$$

so $\hat{\mathcal{H}}$ is

$$\hat{\mathcal{H}} = \varepsilon\left[(1-\xi)\hat{n} + \frac{\xi}{N-1}(P_\tau^\dagger P_\tau + P_\sigma^\dagger P_\sigma + P_\tau^\dagger P_\sigma + P_\sigma^\dagger P_\tau)\right]. \tag{A12}$$

It is straightforward to see that Eqs. (A1) and (A12) are similar. In fact, it can be shown that H' can be written as

$$\begin{aligned} H' = \frac{1}{3\xi+1}\Big[&(1-\xi)n_L + \frac{\xi}{(N-1)}(P_L^\dagger P_L + P_s^\dagger P_s \\ &- P_L^\dagger P_s - P_s^\dagger P_L)\Big], \end{aligned} \tag{A13}$$

with the change,

$$x = \frac{1-\xi}{3\xi+1}. \tag{A14}$$

Comparing Eqs. (A12) and (A13), it is evident that, apart from a global scale $\frac{1}{3\xi+1}$, they are identical except for a couple of signs that correspond to the selection of different pairing operators: In Ref. [30], the pairing (A2) is used, while here, we use the pairing (A11). Apart from a global numerical factor absorbed in the change of the control parameter, both selections correspond to different so(3) realizations, usually called so(3) and $\overline{\text{so(3)}}$ in the literature [19]. These two algebras are isomorphic, and a consistent treatment provides the same results for all matrix elements in the model and, consequently, leads to the same spectra and relevant observables. Thus, the u(3) Hamiltonian used in this paper is a particular case of the boson-pairing Hamiltonian used in Ref. [30], and we have demonstrated here, by an alternative method, that finite-N effects calculated in Ref. [30] are also applied to the case of the L half-integer $L=1/2$ with the change (A14), and properly describe the shape-phase transition in the 2D limit of the molecular vibron model.

[1] R. Gilmore, J. Math. Phys. **20**, 891 (1979).
[2] F. Iachello and A. Arima, *The Interacting Boson Model* (Cambridge University Press, Cambridge, UK, 1987).
[3] F. Iachello and R. D. Levine, *Algebraic Theory of Molecules* (Oxford University Press, Oxford, 1995).
[4] F. Iachello, Rev. Mod. Phys. **65**, 569 (1993).
[5] A. Frank and P. van Isacker, *Algebraic Methods in Molecular and Nuclear Structure Physics* (Wiley, New York, 1994).
[6] F. Iachello and N. V. Zamfir, Phys. Rev. Lett. **92**, 212501 (2004).
[7] P. Cejnar and J. Jolie, Prog. Part. Nucl. Phys. **62**, 210 (2009).

[8] R. F. Casten, Prog. Part. Nucl. Phys. **62**, 183 (2009).
[9] P. Cejnar, J. Jolie, and R. F. Casten, Rev. Mod. Phys. **82**, 2155 (2010).
[10] F. Iachello, Chem. Phys. Lett. **78**, 581 (1981).
[11] F. Iachello and R. D. Levine, J. Chem. Phys. **77**, 3046 (1982).
[12] O. S. V. Roosmalen, A. E. L. Dieperink, and F. Iachello, Chem. Phys. Lett. **85**, 32 (1982).
[13] O. S. V. Roosmalen, F. Iachello, R. D. Levine, and A. E. L. Dieperink, J. Chem. Phys. **79**, 2515 (1983).
[14] O. S. van Roosmalen, I. Benjamin, and R. D. Levine, J. Chem. Phys. **81**, 5986 (1984).
[15] A. Frank, R. Lemus, R. Bijker, F. Pérez-Bernal, and J. M. Arias, Ann. Phys. **252**, 211 (1996).
[16] F. Iachello and S. Oss, J. Chem. Phys. **104**, 6956 (1996).
[17] F. Iachello, F. Pérez-Bernal, and P. H. Vaccaro, Chem. Phys. Lett. **375**, 309 (2003).
[18] F. Pérez-Bernal, L. F. Santos, P. H. Vaccaro, and F. Iachello, Chem. Phys. Lett. **414**, 398 (2005).
[19] F. Pérez-Bernal and F. Iachello, Phys. Rev. A **77**, 032115 (2008).
[20] F. Iachello, Philos. Mag. Lett. **82**, 289 (2002).
[21] F. Pan, Y. Zhang, S. Jin, J. P. Draayer, M.-L. Ge, and J. L. Birman, Phys. Lett. A **341**, 291 (2005).
[22] S. Jin, B. Xie, H. Zhang, J. L. Birman, and M.-L. Ge, Philos. Mag. Lett. **86**, 743 (2006).
[23] M. A. Caprio, P. Cejnar, and F. Iachello, Ann. Phys. **323**, 1106 (2008).
[24] P. Cejnar and P. Stránský, Phys. Rev. E **78**, 031130 (2008).
[25] A. Relaño, J. M. Arias, J. Dukelsky, J. E. García-Ramos, and P. Pérez-Fernández, Phys. Rev. A **78**, 060102(R) (2008).
[26] P. Pérez-Fernández, A. Relaño, J. M. Arias, J. Dukelsky, and J. E. García-Ramos, Phys. Rev. A **80**, 032111 (2009).
[27] F. Pérez-Bernal and O. Álvarez-Bajo, Phys. Rev. A **81**, 050101(R) (2010).
[28] N. F. Zobov *et al.*, Chem. Phys. Lett. **414**, 193 (2005).
[29] M. Winnewisser *et al.*, J. Mol. Struct. **798**, 1 (2006).
[30] S. Dusuel, J. Vidal, J. M. Arias, J. Dukelsky, and J. E. García-Ramos, Phys. Rev. C **72**, 064332 (2005).
[31] J. M. Arias, J. Dukelsky, J. E. García-Ramos, and J. Vidal, Phys. Rev. C **75**, 014301 (2007).
[32] F. Pérez-Bernal, *triat_u3 v. 2.2.1* [http://www.uhu.es/gem/clinux/descargas.php] (2010).
[33] R. Gilmore and D. Feng, Nucl. Phys. A **25**, 189 (1978).
[34] D. H. Feng, R. Gilmore, and S. R. Deans, Phys. Rev. C **23**, 1254 (1981).
[35] R. N. Dixon, Trans. Faraday Soc. **60**, 1363 (1964).
[36] J. N. Ginocchio and M. W. Kirson, Phys. Rev. Lett. **44**, 1744 (1980).
[37] A. Bohr and B. R. Mottelson, Phys. Scr. **22**, 468 (1980).
[38] A. E. L. Dieperink, O. Scholten, and F. Iachello, Phys. Rev. Lett. **44**, 1747 (1980).
[39] H. J. Lipkin, N. Meshkov, and A. J. Glick, Nucl. Phys. **62**, 188 (1965).
[40] O. S. van Roosmalen, R. D. Levine, and A. E. L. Dieperink, Chem. Phys. Lett. **101**, 512 (1983).
[41] O. S. van Roosmalen, Ph.D. thesis, University of Groningen, The Netherlands, 1982 (unpublished).
[42] A. Leviatan and M. W. Kirson, Ann. Phys. (NY) **188**, 142 (1988).
[43] A. Leviatan, Ann. Phys. (NY) **179**, 201 (1987).
[44] M. A. Caprio, J. Phys. A: Math. Gen. **38**, 6385 (2005).
[45] T. Holstein and H. Primakoff, Phys. Rev. **58**, 1098 (1940).
[46] A. Klein and E. R. Marshalek, Rev. Mod. Phys. **63**, 375 (1991).
[47] J. Vidal and S. Dusuel, Europhys. Lett. **74**, 817 (2006).
[48] S. Dusuel, J. Vidal, J. M. Arias, J. Dukelsky, and J. E. García-Ramos, Phys. Rev. C **72**, 011301(R) (2005).
[49] S. Dusuel and J. Vidal, Phys. Rev. A **71**, 060304(R) (2005).
[50] S. Dusuel and J. Vidal, Phys. Rev. Lett. **93**, 237204 (2004).
[51] S. Dusuel and J. Vidal, Phys. Rev. B **71**, 224420 (2005).
[52] M. E. Fisher and M. N. Barber, Phys. Rev. Lett. **28**, 1516 (1972).
[53] R. Botet, R. Jullien, and P. Pfeuty, Phys. Rev. Lett. **49**, 478 (1982).
[54] *Finite Size Scaling*, edited by J. L. Cardy (North Holland, Amsterdam, 1988).
[55] F. Iachello, Phys. Rev. Lett. **85**, 3580 (2000).
[56] F. Iachello, Phys. Rev. Lett. **87**, 052502 (2001).
[57] R. F. Casten and N. V. Zamfir, Phys. Rev. Lett. **85**, 3584 (2000).
[58] R. F. Casten and N. V. Zamfir, Phys. Rev. Lett. **87**, 052503 (2001).
[59] D. J. Rowe, P. S. Turner, and G. Rosensteel, Phys. Rev. Lett. **93**, 232502 (2004).
[60] R. Botet and R. Jullien, Phys. Rev. B **28**, 3955 (1983).